

# Design of ICI Canceling Codes for OFDM Systems Based on Capacity Maximization

Jae Yeun Yun, *Student Member, IEEE*, Sae-Young Chung, *Member, IEEE*, and Yong H. Lee, *Senior Member, IEEE*

**Abstract**—Rate- $t/k$  ( $t \leq k$ ) intercarrier interference (ICI) canceling codes for orthogonal frequency division multiplexing (OFDM) systems are proposed. The capacity lower bounds of OFDM systems employing these codes are derived for time-varying frequency-selective channels. The optimal codes maximizing these bounds are designed numerically. The simulation results indicate that the optimal codes can provide both higher capacity lower bounds and lower bit error rates (BERs) than the existing ICI canceling codes.

**Index Terms**—Capacity, intercarrier interference (ICI), orthogonal frequency division multiplexing (OFDM), time-varying channel.

## I. INTRODUCTION

IT HAS BEEN recognized that the performance of an orthogonal frequency division multiplexing (OFDM) system can be severely degraded by intercarrier interference (ICI) resulting from the channel variation within an OFDM symbol period. To compensate for the ICI, various techniques have been introduced including frequency- and time-domain equalizations (see [1] and references therein), the rate- $1/k$  ICI cancellation schemes [2]–[5], and the frequency-domain partial response coding (PRC) [6], [7]. Among these approaches, the equalizations would be the most common, but their implementation tends to require heavy computation when the channel varies fast. The rate- $1/k$  ICI cancellation schemes based on the use of frequency-domain coding or time-domain windowing are simple and effective; however, these schemes reduce the spectral efficiency by a factor of  $k$ . The PRC does not sacrifice spectral efficiency but often needs the maximum-likelihood sequence estimator (MLSE) to minimize performance loss; thus, this increases the receiver complexity.

In this letter, we propose rate- $t/k$  ( $t \leq k$ ) frequency-domain codes by generalizing the rate- $1/k$  codes in [2] and [3]. The proposed scheme consists of linear transmit and receive codes and is useful for reducing the receiver complexity. Based on the observation that an OFDM system employing the rate- $t/k$  code can be viewed as a collection of multi-input multi-output (MIMO) systems, the capacity lower bound of such an OFDM system is derived. Then, the optimal codes maximizing the lower bound are designed numerically. In the simulation, the

ICI canceling codes are examined in terms of the capacity lower bound and bit error rate (BER).

The following notations are used throughout this letter:  $\text{diag}(\mathbf{A}_0, \dots, \mathbf{A}_{k-1})$  represents a block diagonal matrix whose diagonal blocks are  $\mathbf{A}_0, \dots, \mathbf{A}_{k-1}$ .  $[\mathbf{A}]_{p,q}$  denotes the  $(p, q)$ th element of matrix  $\mathbf{A}$ .  $\otimes$  represents the Kronecker product, and  $\circ$  denotes the Hadamard product.<sup>1</sup>  $\mathbf{I}_t$  stands for a  $t$ -by- $t$  identity matrix, and  $(\cdot)_N$  denotes a modulo- $N$  operation.  $\text{tr}[\cdot]$  stands for matrix trace.

## II. SYSTEM MODEL

Fig. 1 illustrates an OFDM system with the proposed frequency-domain coding. This system employs an  $N$ -by- $M$  block diagonal matrix,  $\Theta = \text{diag}(\mathbf{B}, \dots, \mathbf{B})$ , for transmit coding and an  $M$ -by- $N$  block diagonal matrix,  $\Phi^H = \text{diag}(\mathbf{G}^H, \dots, \mathbf{G}^H)$ , for receive coding, where  $\mathbf{B}$  and  $\mathbf{G}$  are  $k$ -by- $t$  matrices ( $k$  and  $t$  divide  $N$  and  $M$ , respectively), and  $\text{tr}[\mathbf{B}\mathbf{B}^H] \leq k$  is assumed to constrain transmit power. The rate of this transmit/receive coding is  $M/N (= t/k)$ . The received vector  $\mathbf{y}$ , which is  $M$ -dimensional, is given by

$$\mathbf{y} = \Phi^H \mathbf{H} \Theta \mathbf{s} + \Phi^H \mathbf{w} \quad (1)$$

where  $\mathbf{s}$  is the  $M$ -dimensional input vector,  $\mathbf{w}$  is an  $N$ -dimensional additive white Gaussian noise (AWGN) vector, and  $\mathbf{H}$  is the frequency-domain channel matrix defined as  $\mathbf{H} = \mathbf{Q} \mathbf{H}_t \mathbf{Q}^H$ . Here,  $\mathbf{Q}$  is the  $N$ -point discrete Fourier transform (DFT) matrix with  $[\mathbf{Q}]_{p,q} = (1/\sqrt{N})e^{-j(2\pi/N)pq}$ ,  $\mathbf{H}_t$  is an  $N$ -by- $N$  time-domain channel matrix given by  $[\mathbf{H}_t]_{p,q} = h(p; (p-q)_N)$  if  $0 \leq (p-q)_N \leq L-1$ , and 0 otherwise.  $h(n; l)$  represents the  $l$ th tap of the time-domain channel impulse response corresponding to the  $n$ th sample ( $0 \leq n \leq N-1$ ) of an OFDM symbol. If the channel varies within an OFDM symbol duration, the frequency-domain channel matrix  $\mathbf{H}$  has off-diagonal terms causing ICI. The  $N$ -by- $N$  matrix  $\mathbf{H}$  is partitioned into  $k$ -by- $k$  blocks, and the  $(u, v)$ th block is denoted by  $\mathbf{H}(u, v)$ . To rewrite (1) in terms of  $\{\mathbf{H}(u, v)\}$ , vectors  $\mathbf{y}$ ,  $\mathbf{s}$ , and  $\mathbf{w}$  are partitioned as follows:  $\mathbf{y} = [\mathbf{y}^T(0), \dots, \mathbf{y}^T(M/t-1)]^T$ ,  $\mathbf{s} = [\mathbf{s}^T(0), \dots, \mathbf{s}^T(M/t-1)]^T$ , and  $\mathbf{w} = [\mathbf{w}^T(0), \dots, \mathbf{w}^T(N/k-1)]^T$ , where  $\mathbf{y}(u)$  and  $\mathbf{s}(u)$  are  $t$ -dimensional vectors, and  $\mathbf{w}(u)$  is a  $k$ -dimensional vector. Then, the  $u$ th block of  $\mathbf{y}$  in (1) can be expressed as

$$\begin{aligned} \mathbf{y}(u) &= \mathbf{G}^H \mathbf{H}(u, u) \mathbf{B} \mathbf{s}(u) \\ &\quad + \sum_{v=0, v \neq u}^{N/k-1} \mathbf{G}^H \mathbf{H}(u, v) \mathbf{B} \mathbf{s}(v) + \mathbf{G}^H \mathbf{w}(u) \\ &\triangleq \mathbf{G}^H \mathbf{H}(u, u) \mathbf{B} \mathbf{s}(u) + \mathbf{v}(u) \end{aligned} \quad (2)$$

<sup>1</sup>Suppose that  $\mathbf{A}$ ,  $\mathbf{B}$  are matrices of the same size. If  $\mathbf{C} = \mathbf{A} \circ \mathbf{B}$ , then  $[\mathbf{C}]_{p,q} = [\mathbf{A}]_{p,q} [\mathbf{B}]_{p,q}$ .

Manuscript received March 2, 2006; revised August 7, 2006. This work was supported in part by the University Information Technology Research Center Program of the government of Korea. The associate editor coordinating the review of this manuscript and approving it for publication was Prof. Geert Leus.

The authors are with the Department of Electrical Engineering and Computer Science, Korea Advanced Institute of Science and Technology, Daejeon 305-701, Korea (e-mail: yeuny@stein.kaist.ac.kr; sychung@ee.kaist.ac.kr; yohlee@ee.kaist.ac.kr).

Digital Object Identifier 10.1109/LSP.2006.884035

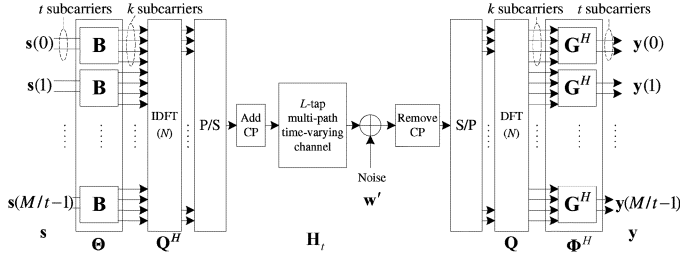


Fig. 1. OFDM system with rate- $t/k$  ICI canceling codes.

where  $\mathbf{v}(u) = \sum_{v=0, v \neq u}^{N/k-1} \mathbf{G}^H \mathbf{H}(u, v) \mathbf{B} \mathbf{s}(v) + \mathbf{G}^H \mathbf{w}(u)$ . Because most of the ICI comes from the nearest subcarriers, the matrices  $\{\mathbf{H}(u, v) | u \neq v\}$  in (2) have many small entries with respect to  $\{\mathbf{H}(u, u)\}$ . When  $t = 1$  ( $\mathbf{B}$  and  $\mathbf{G}$  are  $k$ -dimensional vectors) and  $\mathbf{B} = \mathbf{G}$  whose  $p$ th element is given by  $(-1)^p \binom{k-1}{p}$ , (2) represents an OFDM system with the rate- $1/k$  code in [2] and [3]. In (2), the first and second terms are viewed as the desired signal and interference, respectively, and the  $t$  input symbols in  $\mathbf{s}(u)$  are assumed to be jointly detected at the receiver. Then, the system represented by (2) can be thought of as a MIMO system with transmit and receive coding, corrupted by interference. The code matrices  $\{\mathbf{B}, \mathbf{G}\}$  are designed so that the capacity lower bound of the MIMO system is maximized. At the receiver,  $\mathbf{s}(u)$  in (2) can be detected using the same techniques as for MIMO systems, such as the maximum likelihood (ML) [8] and V-BLAST detectors [9]. Receiver complexity can be controlled by properly selecting the parameter  $t$ , which is a dimension of  $\mathbf{s}(u)$ . Throughout this letter, the diagonal blocks  $\{\mathbf{H}(u, u)\}$  are assumed to be perfectly known at the receiver,<sup>2</sup> while they remain unknown at the transmitter.

### III. CAPACITY LOWER BOUND

The capacity lower bound of the system in (2) is derived under the following assumptions.

A.1) The input  $\mathbf{s}$  and noise  $\mathbf{w}$  are circularly symmetric Gaussian random vectors with the covariances  $\mathbf{R}_s = \mathbf{I}_M$  and  $\mathbf{R}_w = \sigma^2 \mathbf{I}_N$ , respectively.

A.2) All multipaths of the channel are mutually uncorrelated, and each time-domain channel tap,  $h(n; l)$ , is a wide-sense stationary random process having Rayleigh magnitude and uniform phase. Specifically, it is assumed that

$$E[h(n; l)h^*(n'; l')] = \sigma_l^2 r(n - n') \cdot \delta(l - l') \quad (3)$$

where  $r(n) = E[h(m+n; l)h^*(m; l)]/\sigma_l^2$ , and  $\sigma_l^2$  denotes the mean power of the  $l$ th channel tap. It is also assumed that the channel power is normalized to satisfy  $\sum_l \sigma_l^2 = 1$ .

Under these assumptions, the interference  $\mathbf{v}(u)$  in (2) is independent of  $\mathbf{s}(u)$ , and the signal-to-noise ratio (SNR) is given by  $1/\sigma^2$ . The lower bound of the capacity is obtained under the assumption that  $\mathbf{v}(u)$  is Gaussian.<sup>3</sup> (In fact,  $\mathbf{v}(u)$  is not Gaussian because it is a linear combination of products of Gaussian random processes.) Given the covariance

<sup>2</sup>Efficient channel estimation techniques for OFDM systems over time-varying channels have been proposed in [10], [11].

<sup>3</sup>The capacity of a non-Gaussian interference channel is lower bounded by the capacity of a Gaussian interference channel with the same interference covariance [13], [14]. Here the capacity of a Gaussian interference channel is achieved when the input signal is Gaussian.

$\mathbf{R}_{v(u)} = E[\mathbf{v}(u)\mathbf{v}^H(u)]$ , the capacity lower bound of the  $u$ th subsystem represented by (2) is written as [12], [13]

$$C_u = E \left[ \frac{1}{k} \log_2 \det (\mathbf{I}_t + \mathbf{G}^H \mathbf{H}(u, u) \times \mathbf{B} \mathbf{B}^H \mathbf{H}^H(u, u) \mathbf{G} \mathbf{R}_{v(u)}^{-1}) \right] \quad (4)$$

with expectation over the distribution of  $\mathbf{H}(u, u)$ . After the calculations outlined in the Appendix,  $\mathbf{R}_{v(u)}$  is given by

$$\mathbf{R}_{v(u)} = \mathbf{G}^H \tilde{\mathbf{Q}} \left\{ \left( \frac{N}{k} \mathbf{R}'_T - \mathbf{R}_T \right) \otimes (\mathbf{R}_F \circ \mathbf{B} \mathbf{B}^H) \right\} \times \tilde{\mathbf{Q}}^H \mathbf{G} + \sigma^2 \mathbf{G}^H \mathbf{G} \quad (5)$$

where  $\mathbf{R}_F$  is a  $k$ -by- $k$  matrix defined as  $[\mathbf{R}_F]_{p,q} = \sum_{l=0}^{L-1} \sigma_l^2 e^{-j(2\pi/N)(p-q)l}$ ,  $\mathbf{R}_T$  and  $\mathbf{R}'_T$  are  $N$ -by- $N$  matrices given by  $[\mathbf{R}_T]_{p,q} = r(p - q)$  and  $[\mathbf{R}'_T]_{p,q} = [\mathbf{R}_T]_{p,q} \cdot \delta(p - q + m(N/k))$ , respectively, with an arbitrary integer  $m$  (the elements of  $\mathbf{R}'_T$  are selected from those of  $\mathbf{R}_T$ ),  $\tilde{\mathbf{Q}} = [\tilde{\mathbf{q}}_0 \tilde{\mathbf{q}}_0^H, \dots, \tilde{\mathbf{q}}_{N-1} \tilde{\mathbf{q}}_{N-1}^H]$ , and  $\tilde{\mathbf{q}}_n$  is a  $k$ -dimensional vector whose  $p$ th element is given by  $(1/\sqrt{N})e^{-j(2\pi/N)np}$ . Note that  $\mathbf{R}_{v(u)}$  is independent of  $u$ . Therefore, the notation  $\mathbf{R}_v$  will be used instead of  $\mathbf{R}_{v(u)}$ . Furthermore, in (4),  $\{C_u | 0 \leq u \leq N/k - 1\}$  are identical to each other because the distributions of  $\{\mathbf{H}(u, u)\}$  are identical for all  $u$ . In what follows, for simplicity, the subscript  $u$  is set at zero ( $u = 0$ ), and  $C_0$  is considered. If the channel autocorrelation  $r(n)$ , the channel power profile  $\{\sigma_l^2\}$ , and the noise power  $\sigma^2$  (or SNR) are known, then  $\mathbf{R}_v$  can be obtained. However, deriving a closed-form expression of  $C_0$  by evaluating the expectation in (4) turns out to be a difficult task. This expectation will be approximated using Monte Carlo methods in the simulation. Before concluding this section, it is worthwhile to make the following observation.

*Observation 1:* When  $k \ll N$  and  $L \ll N$ , the capacity bound  $C_0$  for a frequency-selective channel ( $L > 1$ ) with  $\{h(n; l) | 0 \leq n \leq N - 1, 0 \leq l \leq L - 1\}$  can be approximated by that for a flat-fading channel ( $L = 1$ ) with  $\{\sum_{l=0}^{L-1} h(n; l) | 0 \leq n \leq N - 1\}$ .

This observation is true because when  $k \ll N$  and  $L \ll N$ ,  $[\mathbf{H}(0, 0)]_{p,q} = (1/N) \sum_{n=0}^{N-1} \sum_{l=0}^{L-1} h(n; l) e^{-j(2\pi/N)ql} e^{j(2\pi/N)(q-p)n} \approx (1/N) \sum_{n=0}^{N-1} \{\sum_{l=0}^{L-1} h(n; l)\} e^{j(2\pi/N)(q-p)n}$ , and  $[\mathbf{R}_F]_{p,q} \approx 1$  for all  $p$  and  $q$ . Since  $k \ll N$  and  $L \ll N$  in practice, the code matrices will be only designed for flat-fading channels.

### IV. CODE DESIGN

The code matrices  $\{\mathbf{B}, \mathbf{G}\}$  are designed so that the capacity bound  $C_0$  is maximized under a transmission power constraint. The optimization problem can be written as

$$\underset{\mathbf{B}, \mathbf{G}}{\text{maximize}} C_0, \text{ subject to } \text{tr}[\mathbf{B} \mathbf{B}^H] = k.$$

Since a closed-form expression of  $C_0$  is not available, this optimization is performed through numerical simulation. The optimization procedure is summarized as follows.

- 1) The channel  $\mathbf{H}(0, 0)$  is generated based on Jakes' model [15] while varying the normalized Doppler frequency  $f_d T_s$  from 0.01 to 0.51 at intervals of 0.05. Here,  $T_s$  denotes the

TABLE I  
OPTIMAL ICI CANCELING CODE MATRICES  $\mathbf{B}$ , WHERE  $\mathbf{B} = \mathbf{G}$

$k = 2, t = 1$	$k = 2, t = 2$	$k = 3, t = 2$
$\begin{bmatrix} 0.5806 \\ -1.2895 \end{bmatrix}$	$\begin{bmatrix} 0.9924 & 0.1193 \\ -0.8183 & 0.5756 \end{bmatrix}$	$\begin{bmatrix} 0.3775 & -0.3992 \\ -1.1724 & 0.1653 \\ 0.5356 & 1.0047 \end{bmatrix}$

OFDM symbol duration. For each  $f_d T_s$ ,  $\mathbf{H}(0, 0)$  is independently generated 20 times.

- 2) The correlation  $r(n)$  is assumed to be the average of  $J_0(2\pi f_d T_s n/N)$  over the  $f_d T_s$  that varies from 0.01 to 0.51, where  $J_0(x)$  is a zeroth-order Bessel function of the first kind.
- 3) Given the set of  $\{\mathbf{H}(0, 0)\}$  generated in step 1, the expectation in (4) is approximated by the average over  $\{\mathbf{H}(0, 0)\}$ , and a constrained nonlinear optimization is performed.

The parameters for the numerical simulation are as follows:  $N = 480$ , SNR = 25 dB, and  $(k, t) \in \{(2, 1), (2, 2), (3, 2)\}$ . Based on Observation 1, only flat-fading channels ( $L = 1$ ) are generated for designing  $\{\mathbf{B}, \mathbf{G}\}$ . During the optimization, both real- and complex-valued  $\mathbf{B}$  and  $\mathbf{G}$  are considered.<sup>4</sup> The results indicate that the maximum value of  $C_0$  can be achieved by the real-valued  $\mathbf{B}$  and  $\mathbf{G}$ , which are identical to each other ( $\mathbf{B} = \mathbf{G}$ ).<sup>5</sup> The optimal code matrices are shown in Table I.

## V. PERFORMANCE COMPARISON

The ICI canceling codes in Table I are examined in terms of the capacity lower bound and BER. In the simulation, to show their robustness, the optimal codes are applied to an environment different from the one for which the codes were designed. Specifically,  $N = 120$  and frequency-selective fading channels consisting of eight taps ( $L = 8$ ) with an equal gain power profile are considered (again, Jakes' model is used for generating this channel). The OFDM systems with the proposed rate-1/2, 2/2, and 2/3 codes, which are referred to as P1, P2, and P3, respectively, are compared with the system employing the rate-1/2 code in [2] ( $\mathbf{B} = \mathbf{G} = [1, -1]^T$ ). The latter system is called Z1. In addition, conventional systems without any ICI canceling codes, denoted by C1 ( $\mathbf{B} = \mathbf{G} = \mathbf{I}_2$ ) and C2 ( $\mathbf{B} = \mathbf{G} = \mathbf{I}_2$ ), and those employing simple rate-1/2 and 2/3 codes in [5] are considered. The simple codes are defined by

$$\mathbf{B} = \mathbf{G} = [0, \sqrt{2}]^T \text{ and } \mathbf{B} = \mathbf{G} = \begin{bmatrix} 0 & -\sqrt{3/2} & 0 \\ 0 & 0 & \sqrt{3/2} \end{bmatrix}^T$$

and are referred to as S1 and S2, respectively. For a fair comparison in the BER simulation, we use 16QAM for C1, C2, and P2, 64QAM for S2 and P3, and 256QAM for S1, P1, and Z1 (these modulations guarantee identical transmission rates). In the BER simulation, the systems with  $t = 1$  (C1, S1, P1, and Z1) employ a conventional receiver consisting of a one-tap frequency-domain equalizer followed by a symbol-by-symbol detector, and those with  $t = 2$  (C2, S2, P2, and P3) employ the V-BLAST

<sup>4</sup>We used "fmincon" in the MATLAB optimization toolbox. For each  $(k, t)$ , optimization was performed 30 times while varying the initial values for "fmincon," and we chose  $\{\mathbf{B}, \mathbf{G}\}$  corresponding to the maximum value of  $C_0$ .

<sup>5</sup>Similar optimization has been performed for AWGN channels with a frequency offset. The results, which are not reported here, indicate that real-valued  $\mathbf{B}$  and  $\mathbf{G}$ , which are not identical ( $\mathbf{B} \neq \mathbf{G}$ ), can maximize  $C_0$ .

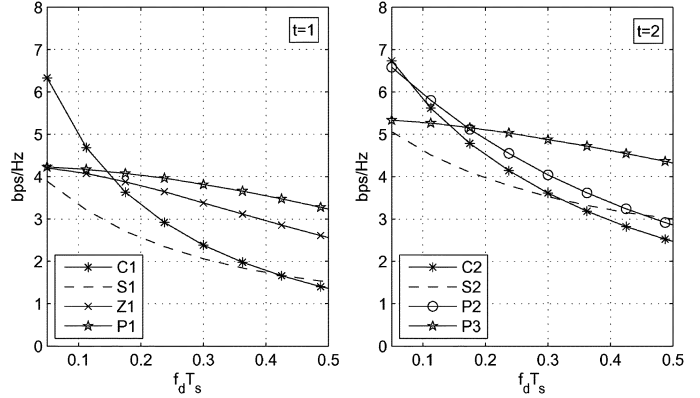


Fig. 2. Capacity lower bound versus  $f_d T_s$  for frequency-selective fading channels when SNR = 25 dB.

receiver. For channel coding, we employ the rate-1/2 convolutional code with a constraint length of 7, along with an interleaver and deinterleaver defined in [16],<sup>6</sup> and perform hard-decision decoding by means of the Viterbi algorithm.<sup>7</sup> The encoding block size is equal to the duration of four OFDM symbols (1920 channel coded bits).

Fig. 2 compares the capacity lower bounds for the frequency-selective channels when SNR = 25 dB. As expected, the capacity lower bounds of the system with C2, S2, and P3, which are two-by-two MIMO systems ( $t = 2$ ), are larger than their counterparts with  $t = 1$  (C1, S1, and P1). Among the ICI canceling codes, the simple codes S1 and S2 perform the worst. They exhibit lower spectral efficiency than C1 and C2 (no coding) unless  $f_d T_s$  is very large. The other ICI canceling codes improve the spectral efficiency for a wider range of  $f_d T_s$ . For example, P1 and P3 can outperform C1 and C2, respectively, when  $f_d T_s > 0.146$ , and P2 can perform better than C2 if  $f_d T_s > 0.078$ . Among the coded systems, with the exception of the simple codes, the capacity of Z1 is less than the others. P2 and P3 exhibit the best performance when  $0.078 < f_d T_s < 0.171$  and  $f_d T_s > 0.171$ , respectively. Therefore, use of either P2 or P3 depending on  $f_d T_s$  may be suggested. Comparing P1 and P2, the latter shows higher spectral efficiency unless  $f_d T_s > 0.353$ . This happened because P2 is a rate-1 code and P1 is a rate-1/2 code that should be more robust to the ICI.

Figs. 3 and 4, respectively, show the coded and uncoded BER for the frequency-selective fading channels when  $f_d T_s = 0.2$ . Due to the ICI, C1, C2, S1, and S2 exhibit an error floor for most SNR values under consideration. Such a severe error floor does not appear in the other coded systems. P3 almost always outperforms the other systems. P1 and Z1 perform better than C1 when the SNR is larger than 17.75 dB. Comparing P1 and P2, the former shows better BER performance than the latter. This is rather surprising because the capacity of P2 is larger than

<sup>6</sup>In [16],  $N = 64$ , and only 48 subcarriers are used for transmission. To consider the case where  $N = 120$  and all the subcarriers are used, the index of the interleaver and deinterleaver was extended.

<sup>7</sup>The assumption that  $\mathbf{s}(u)$  and  $\mathbf{v}(u)$  in (2) are independent tends to remain valid after the channel encoding because the neighboring symbols in  $\mathbf{s}$  are almost uncorrelated due to interleaving, and most of the ICI comes from the nearest subcarriers.

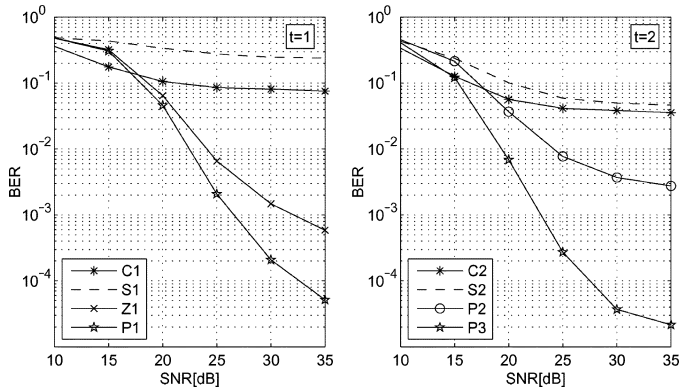


Fig. 3. Coded BER versus SNR for frequency-selective fading channels when  $f_d T_s = 0.2$ .

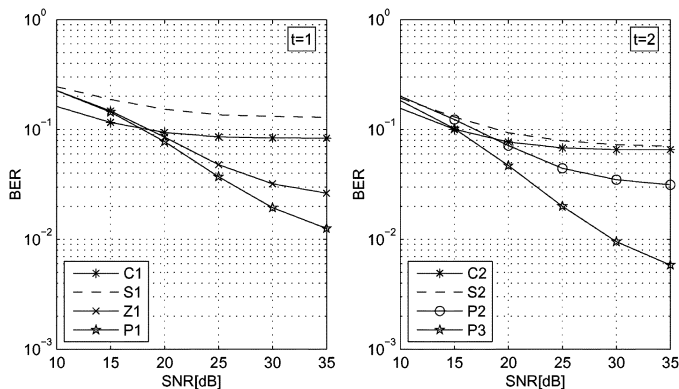


Fig. 4. Uncoded BER versus SNR for frequency-selective fading channels when  $f_d T_s = 0.2$ .

that of P1 when  $f_d T_s = 0.2$  (see Fig. 2). P2 will likely require some optimized transmit/receive processing to improve its BER performance.

In summary, the capacity analysis suggests the use of either P2 or P3 depending on the degree of channel variation. However, P2 tends to exhibit poor BER performance when the transmit/receive processing is not optimized. Therefore, we suggest the use of P3 for systems over fast varying channels.

Finally, it is pointed out that the proposed codes do not cause a severe increase in the computational complexity. Ignoring the matrix multiplications associated with  $\mathbf{B}$  and  $\mathbf{G}$  in (2), the complexity of P1 is identical to that of C1, and P3 causes only a minor increase in complexity due to using the two-by-two V-BLAST detector.

## VI. CONCLUSION

ICI canceling codes for OFDM systems are designed by maximizing the capacity lower bound. The codes proposed in this letter would be useful for systems over fast varying channels with a high SNR. The simulation results suggest using the proposed rate-2/3 code because it can improve the capacity and BER performance while causing only a minor increase in the implementation complexity.

Further research in this area will include the design of transmit/receive processors for the proposed rate 1 codes, such as P2, and the investigation into the reason why the real-valued  $\mathbf{B}$  and  $\mathbf{G}$  maximize  $C_0$ .

## APPENDIX

Under the assumption in A.1),  $\mathbf{R}_{v(u)}$  can be written as

$$\mathbf{R}_{v(u)} = \mathbf{G}^H \mathbf{K}_u \mathbf{G} + \sigma^2 \mathbf{G}^H \mathbf{G} \quad (\text{A1})$$

where  $\mathbf{K}_u = \sum_{v=0, v \neq u}^{N/k-1} E[\mathbf{H}(u, v) \mathbf{B} \mathbf{B}^H \mathbf{H}^H(u, v)]$ . From (3) and the equality  $[\mathbf{H}(u, v)]_{p, q} = 1/N \cdot \sum_{n=0}^{N-1} \sum_{l=0}^{L-1} h(n; l) \cdot e^{-j(2\pi/N)l(kv+q)} e^{j(2\pi/N)(k(v-u)+q-p)n}$ ,  $[\mathbf{K}_u]_{p, q}$  can be written as

$$\begin{aligned} [\mathbf{K}_u]_{p, q} &= \frac{1}{N^2} \sum_{n=0}^{N-1} \sum_{n'=0}^{N-1} r(n-n') \\ &\times \left\{ \frac{N}{k} \delta \left( n-n' + m \frac{N}{k} \right) - 1 \right\} \\ &\times \sum_{s=0}^{k-1} \sum_{s'=0}^{k-1} e^{j \frac{2\pi}{N} (ns - n's')} \sum_{l=0}^{L-1} \sigma_l^2 e^{-j \frac{2\pi}{N} (s-s')l} \\ &\times [\mathbf{B} \mathbf{B}^H]_{s, s'} e^{j \frac{2\pi}{N} (-np + n'q)} \end{aligned} \quad (\text{A2})$$

where  $m$  is an arbitrary integer. Using (A2) in (A1) and converting the resulting equation into a matrix form, we obtain the expression in (5).

## REFERENCES

- [1] L. Rugini, P. Banelli, and G. Leus, "Simple equalization of time-varying channels for OFDM," *IEEE Commun. Lett.*, vol. 9, no. 7, pp. 619–621, Jul. 2005.
- [2] Y. Zhao and S.-G. Haggman, "Intercarrier interference self-cancellation scheme for OFDM mobile communication systems," *IEEE Trans. Commun.*, vol. 49, no. 7, pp. 1185–1191, Jul. 2001.
- [3] J. Armstrong, "Analysis of new and existing methods of reducing intercarrier interference due to carrier frequency offset in OFDM," *IEEE Trans. Commun.*, vol. 47, no. 3, pp. 365–369, Mar. 1999.
- [4] W. T. Ng and V. K. Dubey, "Analysis of PCC-OFDM systems for general time-varying channel," *IEEE Commun. Lett.*, vol. 9, no. 5, pp. 394–396, May 2005.
- [5] A. Seyedi and G. Saulnier, "General ICI self-cancellation scheme for OFDM systems," *IEEE Trans. Veh. Technol.*, vol. 54, no. 1, pp. 198–210, Jan. 2005.
- [6] Y. Zhao and S.-G. Haggman, "Intercarrier interference compression in OFDM communication systems by using correlative coding," *IEEE Commun. Lett.*, vol. 2, no. 8, pp. 214–216, Aug. 1998.
- [7] H. Zhang and Y. Li, "Optimum frequency-domain partial response encoding in OFDM system," *IEEE Trans. Commun.*, vol. 51, no. 7, pp. 1064–1068, Jul. 2003.
- [8] H. Vikalo and B. Hassibi, "On the sphere-decoding algorithm II. Generalizations, second-order statistics, and applications to communications," *IEEE Trans. Signal Process.*, vol. 53, no. 8, pp. 2819–2834, Aug. 2005.
- [9] G. J. Foschini, G. D. Golden, and R. A. Valenzuela, "Simplified processing for high spectral efficiency wireless communication employing multi-element arrays," *IEEE J. Sel. Areas Commun.*, vol. 17, no. 11, pp. 1841–1852, Nov. 1999.
- [10] Y. Choi, P. Voltz, and F. Cassara, "On channel estimation and detection for multicarrier signals in fast and selective Rayleigh fading channels," *IEEE Trans. Commun.*, vol. 49, no. 8, pp. 1375–1387, Aug. 2001.
- [11] A. Stamoulis, S. Diggavi, and N. Al-Dhahir, "Intercarrier interference in MIMO OFDM," *IEEE Trans. Commun.*, vol. 50, no. 10, pp. 2451–2464, Oct. 2002.
- [12] A. Lozano and A. M. Tulino, "Capacity of multiple-transmit multiple-receive antenna architectures," *IEEE Trans. Inf. Theory*, vol. 48, no. 12, pp. 3117–3128, Dec. 2002.
- [13] B. Hassibi and B. M. Hochwald, "How much training is needed in multiple-antenna wireless links?," *IEEE Trans. Inf. Theory*, vol. 49, no. 4, pp. 951–963, Apr. 2003.
- [14] S. Ihara, "On the capacity of channels with additive non-Gaussian noise," *Inf. Control*, vol. 37, pp. 34–39, Sep. 1978.
- [15] W. C. Jakes, *Microwave Mobile Communications*. New York: Wiley, 1974.
- [16] *Part II: Wireless LAN Medium Access Control (MAC) and Physical Layer (PHY) Specification-High-Speed Physical Layer in the 5 GHz Band*, IEEE Std. 802.11a, LAN/MAN Standards Committee, 1999.